July, 2014 第14期

醫工學會

http://www.bmes.org.tw/

中華民國生物醫學工程學會

Taiwanese Society of Biomedical Engineering **E-Newsletter**

P6 活動專欄
2014醫工創意競賽

P1 恭賀！徐善慧教授及研究團隊同時榮獲103年度中工會傑出工程教授與工程論文獎

P17 103年醫工證書考試相關訊息

更多醫工動態盡在醫工學會電子報，請即刻閱讀！
學會為了嘉惠醫工大家庭，100年4月回復電子報發行，預計每三個月出刊一期，敬請期待，對於本學會電子報，有任何意見，歡迎來電指教
(06) 2760665

目錄

醫工學會秘書處：70101 台南市大學路一號
國立成功大學生物醫學工程系轉醫工學會
TEL: +886-6-2760665
FAX: +886-6-2343270
E-mail: tsbme@conf.ncku.edu.tw

【成果榮譽】

恭賀本會生物醫學工程學刊年度優良論文「Enhanced migration of whatron's jelly mesenchymal stem cells grown on polyurethane nanocomposites」榮獲中國工程師學會103年度工程論文獎，獲獎者為：徐善慧教授研究團隊。
詳請請見中國工程師學會103年度各獎項得獎名單：
http://www.cie.org.tw/news_detail.php?id=121

【成果榮譽】

恭賀本會監事徐善慧教授榮獲中國工程師學會103年度傑出工程教授。
詳請請見中國工程師學會103年度各獎項得獎名單：
http://www.cie.org.tw/news_detail.php?id=121

【學會核予教育學分公告】

本會於2014下半年舉辦核予教育學分之活動及研討會如下表所示，敬邀各位醫工先進以及同仁踴躍參與。

日期	活動名稱	地點	主要學分	輔助學分
2014/8/15	2014 生物醫學工程研討會：醫學工程專業人員在醫院的定位及工作範疇之探討	台北	8	X
2014/10/9-12	第9屆亞太生物醫學工程會議暨第1屆全球生物醫學工程會議	台南	30	X
2014/12/13	2014 科技部工程司醫工學門成果發表會暨生物醫學工程及醫材產業高峰論壇	台北	8	X

註：擷取至2014年7月7日，教育學分相關最新公告可至醫工學會網站-研討會專區查詢 http://www.bmes.org.tw/seminar.php

【醫工學會 2014 醫工科技研討會和會員大會說明】

醫工學會下半年度重要年度會議和歷年差別甚大，學會特藉此說明，敬邀及提醒各位醫工先進及同仁予以特別留意，兩項會議安排如下：

GCBME/APCMBE 2014：

會議日期：103 年 10 月 9 至 12 日
會議地點：台南市國立成功大學校區
繼續教育學分：30 主要學分
註：GCBME 2014 係本學會今年唯一主辦的醫工科技研討會，請參酌本會議的詳細說明。

科技部醫學工程學門成果發表會、中華民國生物醫學工程學會會員大會暨理監事改選：

會議日期：103 年 12 月 13 日
會議地點：國立陽明大學校區
繼續教育學分：8 主要學分

說明：

1. 學會發行之學刊(Journal of Medical and Biological Engineering, JMBE)多年來已經獲得 EI 和 SCI 的 index，影響係數和國際投稿量均進步迅速，儕身於國際學術期刊之林。對於推動台灣生物醫學工程國際化的進展，貢獻顯著。

2. 為進一步推動研討會的國際化進程，學會歷經多次理監事會議的討論，於去年決議將年度醫工科技研討會的進行模式改為：一年以全英文國際研討會規格，次年回復以往之中文年度研討會，交替舉辦。全英文國際研討會之名稱為：Global Conference on Biomedical Engineering, GCBME；中文年度研討會仍維持為：生物醫學工程科技研討會。

3. 學會於 2008 年獲得 2014 亞太醫工研討會(2014 Asian Pacific Conference on Medical and Biological Engineering, APCMBE 2014)的主辦權，APCMBE 2014 隸屬國際生物醫學工程聯盟(International Federation for Medical and Biological Engineering, IFMBE)的會議。目前 APCMBE 2014 已獲得 IFMBE 前任、現任、及下任理事長和秘書長的支持，將於會議期間，同時召開 IFMBE 的各項重要會議。所以屆時將有全世界眾多國際醫工組織、專家、學者同時來台，對國際化的交流與提升，將是一個絕佳的機會和場合。

4. 期望一舉打響第一屆 GCBME 的國際知名度，學會決定順勢聯合 APCMBE 2014。因此，GCBME/APCMBE 2014 是學會本年度唯一主辦的醫工科技研討會。敬請所有醫工會員、專家學者、學生、產業界，一起共同來參與學會歷史上第一次的國際研討會。

會議重要日程以及註冊費重要資訊如下：

重要日程	
開放線上註冊	2014/07/01
論文接受通知	2014/07/21
論文修改截止	2014/08/01
註冊優惠截止	2014/08/15
會議日期	2014/10/09-12

台灣區註冊費收取標準：由於歷年參加醫工科技研討會人數眾多，且本會議已爭取到相關政府單位補助，國內專家學者將符合 APCMBE 的優惠註冊費，收費標準如下表：（單位: 新台幣）

	早鳥優惠 Before August 15, 2014	After August 15, 2014
學會會員	6300	6800
非學會會員	7800	8400
學生身分學會會員	1600	1900
學生身分非學會會員	1800	2100

註: 學生身分註冊者可參加 10 月 9 日台南飯店之歡迎晚宴（價值新台幣 600 元），如要參加 10 月 11 日長榮桂冠酒店之晚宴，繳費時需另外付費新台幣 1500 元。

GCBME / APCMBE 2014 會議網址：http://conf.ncku.edu.tw/apcmbe9/

下載會議海報

【2014 第三屆醫工盃】

2014 年第三屆全國大專院校醫工盃聯誼賽已在 6 月 28 日至 6 月 29 日於國立成功大學順利展開並且圓滿結束。
各項球賽結果如下，恭喜以下隊伍以及選手：

	冠軍	亞軍	季軍	殿軍
男子籃球	元培科大	清華大學 A	清華大學 B	
女子籃球	義守大學	清華大學		
男子排球	清華大學	中原大學	義守大學	
女子排球	清華大學	成功大學 A	義守大學	
羽球團體	台灣大學	弘光科大	清華大學	
桌球團體	義守大學	清華大學 B	清華大學 A	
網球團體	成功大學 A	清華大學	成功大學 B	
羽球個人	黃炳逢(成大)	林鈞育(弘光)	張哲耀(弘光)	鄭智原(弘光)
桌球個人	洪道涵(義守)	江俊儒(義守)	錢重億(義守)	趙崑壹(清大)


2014 第三屆 醫工盃在成大


2014 第三屆 醫工盃在成大


2014 第三屆 醫工盃在成大
2014 第三屆 醫工盃在成大


2014 第三屆 醫工盃在成大
2014 第三屆 醫工盃在成大


2014 第三屆 醫工盃在成大

2014 中華民國生物醫學工程創意競賽

「2014 中華民國生物醫學工程創意競賽」決賽已於 103 年 5 月 20 日假南部科學園區—高雄園區熱烈展開並圓滿落幕。32 支參賽隊伍經主辦單位評審團討論決議，總共遴選出特優 1 隊、優等 1 隊、最佳創意獎 1 隊、最佳潛能獎 1 隊以及佳作 8 隊。

創意競賽召集國內各大專院校從事生物醫學工程研究之年輕學子與團隊(大專生及碩博士生)。藉由創意競賽活動，將這群優秀之產業未來人才，聚集於南部科學園區，能直接與園區內之廠商進行人才媒合，達到互相了解並吸引產業優秀人才進駐園區之目的。

本屆競賽所達到之功能：

1. 邀集科技部南部科學園區內廠商參觀且幫助其能有效掌握生物醫學工程之學術研究成果。
2. 促成科技部南部科學園區內廠商能有效的接洽、會談、研討與媒合國內重要學術研究領域之頂尖研究團隊。
3. 吸引國內優秀年輕生物醫學工程人才，樂意投入南部科學園區之生物聚落廠商就業。
4. 藉助此項全國性之競賽活動，拓展南部科學園區生醫聚落知名度。

特優獎項由國立台灣科技大學與國立中央大學合作的隊伍「創新性手術後人工膝關節磨耗與偏為位三維分析及顯示系統」拿下。優等獎、最佳創意獎、最佳潛能獎皆由國立成功大學團隊獲得，囊括三項大獎。獲獎作品將於 103 年 10 月 9 日至 12 日由本會與國際生物醫學工程聯盟(IFMBE)共同主辦之「第一屆全球生物醫學工程會議暨第九屆亞太生物醫學工程會議(GCBME 2014 & APCMBE)」進行作品展示，並頒發獎牌與獎金，亞太生物醫學工程會議將吸引 50 家以上相關國內外廠商及 1200 位以上國內外學者參加。

活動剪影

1. 2014生物醫學工程創意競賽大會主席台

2. 參賽隊伍報到及現場作品佈置

3. 報到台評審委員與貴賓簽到

4. 大會開幕—南科管理局陳俊偉局長致詞

5. 大會開幕—金工中心伏和中執行長致詞

6. 大會開幕—醫工學會蘇芳慶理事長致詞

7. 大會開幕參加貴賓

8. 大會主持人宣布開始評審


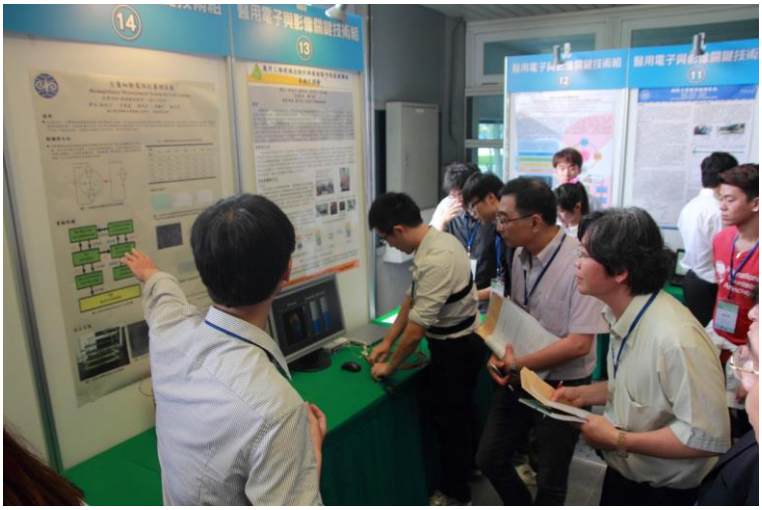

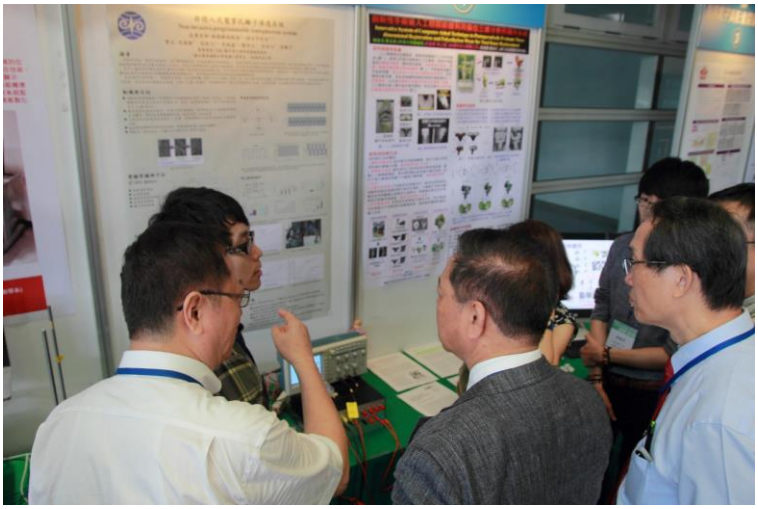
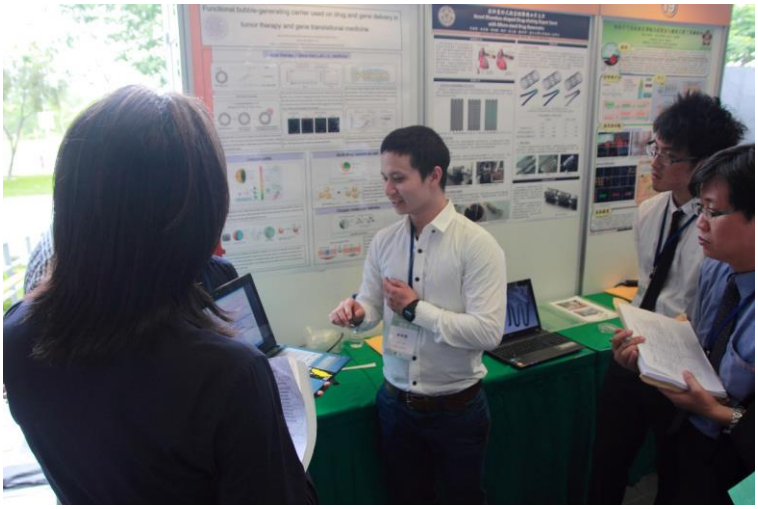
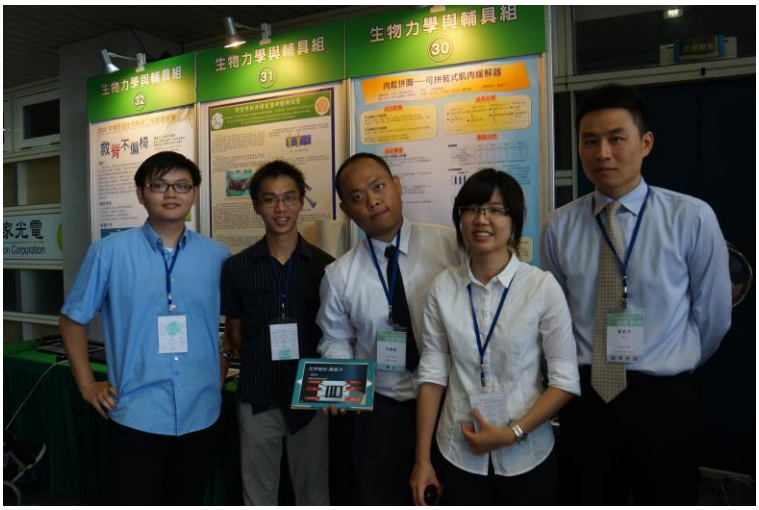

9. 決賽與評審委員評選實況

獲獎隊伍名單

獎項	題目
特優	**創新性手術後人工膝關節磨耗與偏位三維分析及顯示系統** 陳俊名[1] 駱主安[1] 指導教授：林上智[2] 許啟彬[2] [1]中央大學機械工程研究所 [2]台灣科技大學醫學工程研究所
優等	**結合超音波系統與針頭引導於輔助靜脈注射** 劉子傑 黃昱仁 指導教授：王士豪 成功大學資訊工程研究所
最佳創意獎	**免貼片可長效經皮傳輸流感疫苗之鑲嵌式幾丁聚醣微針** 凌銘鴻 林佶民 詹皓安 陳淑媛 李岳瑋 指導教授：陳美瑾 成功大學化學工程學系
最佳潛能獎	**肉鬆拼圖--可拼裝式肌肉緩解器** 王以安 許朝俊 吳佳芸 羅浩倫 指導教授：黃執中 成功大學生物醫學工程學系
佳作	**新型骨折外固定器研發與試製** 江俊儒[1] 陳睿献[1] 陳育駿[1] 許焜翔[1] 蔡柏林[1] 指導教授：林鼎勝[1] 馬景侯[2] [1]義守大學生物醫學工程學系 [2]義大醫院骨科部
佳作	**用於射頻燒灼即時監控之超音波參數影像系統** 馬祥洋[1] 洪傑銘[1] 王蕎茵[1] 李勁緯[1] 指導教授：崔博翔[1] 舒宇宸[2] [1]長庚大學醫學影像暨放射科學系 [2]成功大學數學系
佳作	**健康把關者-生理資訊智慧衣** 蔡宗佑[1] 游坤明[1] 張庭瑄[2] 指導教授：趙一平[1] 徐良育[2] [1]長庚大學資訊工程學系 [2]中原大學生物醫學工程學系
佳作	**應用三維建模技術於肺癌術後呼吸復健輔助系統之開發** 陳亮宇 林沛辰 蘇倩鈺 林以鎬 指導教授：蕭子健 交通大學生物醫學工程研究所
佳作	**玻尿酸/聚己內酯加奈米銀的核/殼奈米纖維膜以達抑菌及抗肌腱沾黏之雙重功能** 陳世賢 李品臻 王馨翊 馮詩婷 指導教授：陳志平 陳志豪 長庚大學化工與材料工程系所
佳作	**開發以奈米碳管繩提供微電流刺激促進神經幹細胞分化及成熟之裝置平台** 葉佳偉 謝舜祐 黃尤傑 指導教授：王子威 清華大學材料科學工程學系
佳作	**全金螢光共振能量轉移新系統模式作為近紅外光對比劑應用在早期骨關節炎診斷** 李之昀 林佳慧 指導教授：王志光 高雄醫學大學醫藥暨應用化學系
佳作	**顱微血管半自動吻合手術器械** 黃少甫 呂明憲 林哲宇 指導教授：林峻立 陽明大學生物醫學工程學系

中華生物醫學工程商業協進會——

整合”醫工商會”資源，開拓醫療生技產業的交流平台

2014/06/30　文/林芝　圖/醫工商會提供

2014/01/04中華生物醫學工程商業協進會成立大會

2014年1月4日由一群台灣生物醫學工程系所畢業的資深產業經理人，為提振台灣生物醫學產業的發展，從產、學、研、醫等不同領域凝聚而成的社團實體『中華生物醫學工程商業協進會』(以下簡稱醫工商會)已誕生了！會中立法院洪秀柱副院長、陳歐珀立法委員，行政院智慧財產局王美花局長、衛生福利部食品藥物管理署（TFDA）醫粧組劉麗玲組長、中原大學工學院李夢輝院長、中華民國放射線醫學會郭萬祐理事長、亞洲腹部放射線醫學會周宜宏理事長、高雄市醫療器材商業同業公會黃金塔理事長、中原大學醫學工程系張恆雄教授、中原大學醫學工程系蔡育秀主任，及各界先進產、官、學、研、醫等嘉賓蒞臨指導與鼓勵，策勵商會能致力於促進醫工產業發展之專業顧問平台，以期為我國生醫產業之發展能有所貢獻。

葉宗仁理事長積極投入社會公益

創會理事長葉宗仁

創會理事長葉宗仁是中原生物醫學工程系第七屆畢業的資深「醫工人」。畢業後即踏入醫療儀器界，憑著「初生之犢不畏虎」的雄心壯志，跟著先輩學習銷售。因為工作態度非常積極，加上衝勁十足，逐漸在醫療產業界累積好名聲，是為醫療界熟悉人稱查爾斯王子的 ”Charles葉”。

一路由本土代理公司轉任美商HP惠普公司、美商安捷倫公司以至荷商飛利浦公司擔任醫療健康事業部總經理。深信大前研一在《後五十歲的選擇》一書所說「人過50要Reset.....」的概念，葉宗仁秉持著台灣醫工人回饋鄉里的信念，毅然決然地自服務20幾年的外商總經理職務，提前退休，並積極地投入社會公益。

葉宗仁說，他的人生前三分之二奉獻給外商公司，他想要趁還有動力以及對醫療市場的熟悉與熱情，選擇「改變」。除擔任中華民國生物醫學工程學會副理事長外，另積極籌組醫工商會，準備為醫療生技產業打造一個資源整合的平台。

導入正確且適當的產業領域

葉宗仁敘述台灣的「生物醫學工程」始創於民國61年，由當時中原理工學院韓偉院長創立醫學工程系，至今42載，畢業系友達三千多人。現今，台灣由北到南與生物醫學工程相關的系所，已然有28個院所，每年畢業專業人員將近千人。然台灣市場有限，生物醫學工程畢業的專業人員實難有發揮的舞台。國際市場雖然蓬勃，但卻也不乏競爭者，本土產業單打獨鬥也難以開拓國際市場。如何將這麼多的生物醫學工程專業人員，導入正確且適當的產業領域以發揮，正是當前的重大課題。

葉宗仁分析隨著世界潮流的進步，再加上各國政府對生物科技的重視程度日增，「生物醫學工程」成為閃亮的明日之星。近年來，因應節能減碳、人口老化、創意經濟等全球趨勢，借助我國資通訊產業的厚實基礎，行政院自民國 98 年 3 月起陸續規畫推動「六大新興產業」及「新興智慧型產業」行動方案，以期創造我國下一波產業契機。而其中「生物科技」與「醫療照護」被列為其中兩項新興產業之中。

台灣社會目前老年人口增加，醫療需求轉為治療與照護並重，此外社會經濟漸趨成熟，對醫藥及醫療服務之購買力增加，醫療照護分工逐漸專業化，創造大量人力需求，形成其相當市場規模及產值的新興產業。

「三個臭皮匠勝過一個諸葛亮」，葉宗仁堅信團結力量大的理念。雖是老掉牙的話，但卻也是歷久不衰的經典名言，放諸四海皆準。成立「中華生物醫學工程商業協進會」的目的，正是有意識的把這些人才整合到這個組織下，進行互相的交流。為了融入兩岸及國際的生技醫療市場醫工商會特地以 Chinese Business Association of Bio-Medical Engineer 為名，葉宗仁說明 Chinese 的中文亦即「中華」，醫工商會將不限於台灣、兩岸，亦將擴及國際的華人世界，希望能同心合作，以提升國內生物醫學工程產業的蓬勃發展，並活躍於國際的醫療產業市場。

入會資格要求嚴格且專業

目前醫工商會已登記有的一百多位成員，其中不乏臨床醫師、臨床醫學工程師、學術教授、財經、資訊等專業人員，並有近百位醫療產業菁英，包括多位醫療製造業負責人及多位國內外資深專業經理人，陣容相當堅強。將所謂的產、學、研、醫大結合，印驗醫工商會目的於連結生技醫療產業、行銷通路，建立整合各界力量。醫工商會的企圖正是要成立這個專業的人力資源整合平台，進一步提供有志於此的通路業、製造業、投顧業，即政府單位專業的顧問平台。

「我們對於會員的入會資格要求嚴格且專業，個人會員必須是醫學工程系、所畢業，在醫療生技產業市場從業達10年以上，並為公司主管或負責人。」葉宗仁表示經由多位志同道合的夥伴多方的努力及認同，我們在短暫的幾個月將一個突發理想變成實質的社團實體，「中華生物醫學工程商業協進會」是為內政部正式登記的非營利社會團體。主要目的為結合生物醫學工程產業經營管理資深人員，合縱連橫，經驗交流，創造結盟商機，以促進生物醫學工程產業的蓬勃發展。進而，與生物醫學工程產、官、學、研單位就醫療生技產業發展彼此交流，以期能提升本土生物醫學工程產業活絡於兩岸醫療生技市場，甚而發揚於國際的醫療產業為目的。

開創更寬廣的職場保障

為了活絡於兩岸國際的醫療生技市場，醫工商會日前正積極的籌辦例會活動及醫療工廠參訪，並拜會各生物醫學工程產、官、學、研單位，包含上海、北京等相關機構。藉此讓生物醫學工程產業前輩和中生代醫工專業人才進行經驗交流，創造求職、求才的供需機會期能合縱連橫，開創生物醫學工程的醫療產業商機。我們且企盼中華生物醫學工程商業協進會的努力能為台灣生物醫學工程學系的下一代開創更寬廣的職場保障！

BME 醫工商會之聲 2014 年 6 月 28 日

THE SOUND OF BIZBME / 發行：中華生物醫學工程商業協進會 / 理事長：葉宗仁 / 民國一百零三年第二季

醫工商會活動報導

輕鬆愉快的參訪活動

2014 年 6 月 13 日（星期五）是醫工商會本年度的第一次參訪活動，本次活動主題是醫療儀器研發製造工廠，參訪目的地是坐落於新竹市附近貴美像理事創立的【聲博科技股份有限公司】及徐源財理事設立的【厚美德生物科技股份有限公司】。

賀 本會 葉宗仁理事長當選 台灣海峽兩岸醫事交流協會 第二屆理事。

醫工商會 103 年第二次例會活動

時間	內容	主講者
11:30~12:00	報到及資料領取	秘書處
12:00~13:00	會員餐會	秘書處
13:00~13:10	理事長致辭	葉宗仁
13:10~14:00	專題演講- 政策與創新—醫療產業新趨勢	洪子仁總經理
14:00~14:30	會員分享- 實戰式中央監護系統在長照中心及普通病房的運用	盧智成執行長
14:30~15:00	會員分享- 長期照顧發展趨勢下醫工產業的利基	陳納堯執行長
15:00~15:40	工商服務時間- 工商服務報告及摩比泰斯移動科技分享	陳皇銘
15:40~15:50	會員互動時間，散會	

台灣海峽兩岸醫事交流協會

依醫工商會第一屆第二次理事會決議通過，本商會已加入台灣海峽兩岸醫事交流協會是為團體會員。

中華生物醫學工程商業協進會秘書處編輯 商會網址：www.bizbme.org 1

103 年醫工證書考試相關訊息

本會將於 2014 年 8 月 2 日(六)舉行本年度之臨床工程師、醫療設備技師、醫學工程師之醫工證書考試。非會員報考者，亦可參加考試。待考試通過後，必須完成入會申請並審核通過，始頒予證書。入會相關規定請至學會網站進入「各式辦法與表格下載區」，參考「中華民國生物醫學工程學會會員入會申請須知」(http://www.bmes.org.tw/down_list.php)。

本次醫工證書考試報名已於 103 年 7 月 1 日截止，報名統計預計今年將有 247 名考生參加證書考試。考試結果將於 8 月底以專函個別通知並公佈於學會網站上。最新證書考試訊息，請至醫工學會網站查詢。

- **筆試日期：2014 年 8 月 2 日（六） 上午 09:30-11:30**
- **口試日期：2014 年 8 月 2 日（六） 下午 13:30-17:00**
- **考試地點：私立中原大學工學館（桃園縣中壢市中北路 200 號）**

2014 Vol. 34, No. 2

Review: Optical Scanning Probe for Optical Coherence Tomography

Chia-Wei Sun, Shyh-Yuan Lee, Kun-Feng Lin

Optical coherence tomography (OCT) has become an important medical imaging modality. However, low penetration depth limits its application. Therefore, the optical scanning probe plays an important role in OCT systems for clinical applications. This article reviews OCT methodology and the mechanisms of an optical scanning probe. Recent developments of OCT probe and related clinical applications are summerized. Various OCT probe techniques (e.g., side imaging and forward imaging) have been used for measuring optical biopsy of various tissues. OCT probes for early diagnosis applications should be developed and combined with functional OCT modalities, such as Doppler OCT and polarization-sensitive OCT, to provide more information for diagnosis.

Effects of Fluid Dynamic Forces Created by Rotary Orbital Suspension Culture on Cardiomyogenic Differentiation of Human Embryonic Stem Cells

Akimi Mogi, Shunsuke Takei, Hisashi Shimizu, Haruki Miura, Daihachiro Tomotsun, Katsunori Sasaki

Human embryonic stem cells (hESCs) have the potential to become an effective resource for regenerative medicine in heart disease. The efficiency of cardiomyocyte differentiation changes drastically depending on the quality of hESC aggregates known as embryoid bodies (EBs). This study compares the production of EBs in rotary orbital suspension culture at various speeds with that in a simple static suspension culture. None of the outgrowths of EBs formed in static suspension culture developed beating. In contrast, outgrowths from EBs formed at 100 rpm had the highest rate of beating, 70%, and increased the expression of Nkx2.5, a master gene of cardiomyocyte differentiation. Outgrowths from EBs developed at slower rotational speeds showed more endoderm gene expression. At faster speeds, the expression of ectoderm markers increased. A computational hydrodynamic simulation showed that the liquid medium shear stress on the bottom was restricted to the periphery at 30 and 55 rpm and the center at 120 rpm. The analysis showed that at 100 rpm, the shear stress was uniformly distributed in the dish. Our results suggest that shear stress by fluid dynamic forces induces the differentiation of specific cell phenotypes from hESCs depending on rotational speed. For cardiomyocyte differentiation, 100 rpm was the most effective speed.

Surface Microstructure and Bioactivity of Hydroxyapatite and Fluorapatite Coatings Deposited on Ti-6Al-4V Substrates Using Nd-YAG Laser

Chi-Sheng Chien, Tze-Yuan Liao, Ting-Fu Hong, Tsung-Yuan Kuo, Chih-Han Chang, Min-Long Yeh, Tzer-Min Lee

Hydroxyapatite (HA) and fluorapatite (FA) coatings were deposited on Ti-6Al-4V substrates with an Nd-YAG laser and then immersed in simulated body fluid (SBF) for up to 21 days to evaluate their bioactivity. Prior to SBF immersion, the coating layer of the HA specimen had a coral-like structure, and was mainly composed of Ti, CaTiO3, TiO2, Al2O3, and Ca2P2O7, whereas that of the FA specimen had a dense cellular-like structure, and was mainly composed of Ti, CaTiO3, TiO2, Al2O3, and residual FA. The Ca/P ratios of the HA and FA coating layers were 7.61 and 2.12, respectively. After 21 days of immersion in SBF, only a very small amount of precipitates, mainly consisting of CaCO3 with some hydroxycarbonated apatite (HCA) and HA, formed on the HA coating layer, whose Ca/P ratio retained a high value of 6.34. In contrast, a dense accumulation of granulated precipitates, mainly consisting of HCA, formed on the FA coating layer after just 7 days of SBF immersion, with a corresponding Ca/P ratio of 1.63. The SBF immersion test shows that FA coatings produced via an Nd-YAG laser cladding technique on a Ti-6Al-4V substrate have better bioactivity than that of their HA counterparts.

Impingement Analysis with 3-D Geometric Characterizations of ACL Pseudofibers and Intercondylar Notch

David T. Fung, Song Joo Lee, Yupeng Ren, Sang Hoon Kang, Shu Q. Liu, Li-Qun Zhang

Impingement of the anterior cruciate ligament (ACL) against the intercondylar notch (ICN) may play a significant role in ACL injuries. However, there is a lack of convenient and accurate methods for evaluating ACL impingement with consideration of the three-dimensional (3-D) notch shape and ACL fibers. In the current study, ACL impingement was modeled using a 3-D geometric knee model that includes multiple ACL pseudofibers, which allowed us to identify the sites of ACL impingement during simulated tibiofemoral movements. The simulation results were compared with impingement force data measured in three cadaveric knees with ACL impingement. Results show that ACL impingement can occur on fibers at the anterolateral aspect of the anteromedial band of the ACL during tibial external rotation and abduction. The computed peak ACL strains of the three knees were 5-8%. The proposed analysis is a practical method for quantitatively evaluating ACL impingement against the ICN, and may lead to useful tools for evaluating ACL impingement in individual patients based on their magnetic resonance imaging data. These analytical tools may guide individualized rehabilitation and reduce potential ACL impingement against the ICN during strenuous tibiofemoral movements.

Comparison of Kinetic Roles of Digits in Two Jar Twisting Directions among Young Females

Chen-Yu Huang, Li-Chieh Kuo, Sheng-Kun Chang, Fong-Chin Su

The jar opening movement requires a complex integration of digits and adequate grasp strength. Unfortunately, many young females have difficulty achieving this task. The opening direction may be an important element related to the force efficiency of hand. However, few studies have been conducted on this topic with an actual human movement. The purpose of this study was to investigate the effect of jar twisting direction on hand kinetics during a maximum voluntary twist. It was hypothesized that changing the twist direction would alter the results of hand kinetics and that an optimal twist direction could be found for opening a jar. Thirty-six healthy young females with mean age, body weight, and height of 23.5 ± 3.6 years, 53.1 ± 6.0 kg, and 160.4 ± 4.3 cm, respectively, were recruited. A custom jar instrument was fabricated to record the kinetics of hand and digit groups. All participants performed jar twisting movements in the clockwise and counterclockwise directions. The results showed that the overall torque and resultant force of right hand increased when a clockwise twist was applied. The resultant force and torque shares of the thumb also increased for the clockwise twist even though those of the middle-ring-little digit group showed no difference and those of the index digit decreased. The index digit and thumb contributed the least and most effort, respectively, for both twisting directions. The thumb was the main force digit. Normal force was the main component of force for all digit groups. The force projections showed that other digit groups not only antagonized the thumb but also one another. The results supported the hypothesis that there were kinetics differences for digits for the two twisting directions. Jar lids could be opened more efficiently in the clockwise direction and kinetics of each digit group also provided as a precursor to jar design modification.

Dynamic Distribution of Cells in Porous Scaffolds During Cell Loading

Qianqian Han, Chao Li, Haifeng Liu, Boon Chin Heng, Gang Wu, Zigang Ge

Little is known about the cell loading process, as the majority of tissue engineering studies focus on relatively long time points. The present study investigates the dynamic distribution of cells during the initial cell loading process in porous scaffolds, namely those made of type-I collagen and silk fibroin, with similar porosities and pore sizes. Loading efficiency of the cells was higher in the silk fibroin scaffold (90%±1.8%) compared to that in the type-I collagen scaffold (76%±1.0%). There were significantly more unattached cells in the type-I collagen scaffold at 0.5 h compared to those in the silk scaffold ($p = 0.03$). The number of adherent cells decreased with time in the type-I collagen scaffold ($p = 0.01$), whereas in the silk scaffold, the loading cells gradually attached to the biomaterials or aggregated with time. The majority of the cells gradually attached to the scaffolds within 6 h and exhibited an elongated morphology, which did not change. In general, there was no significant difference in cell adhesion and cell morphology between the two types of scaffold. The initial six hours were critical for the cell seeding process.

Application of Prediction and Multiscale Synchronization to Brain-Computer Interface

Wei-Yen Hsu

This study proposes an electroencephalographic (EEG) analysis system for brain-computer interface applications. With the combination of neuro-fuzzy prediction, multiscale synchronization features are applied for feature extraction in motor imagery (MI) analysis. The features are extracted from EEG signals recorded from subjects performing left and right MI. Time-series predictions are performed by training two adaptive neuro-fuzzy inference systems for respective left and right MI data. Features are then calculated from the difference of multiscale coherence and phase-locking-value features between the predicted and actual signals through a window of EEG signals. Finally, a support vector machine classifier is used for classification. The performance of the proposed system is compared to that of two popular approaches on six subjects from two data sets. The results indicate that the proposed system is promising for MI classification.

Effects of Anterior Ethmoidectomy with and without Antrotomy and Uncinectomy on Nasal and Maxillary Sinus Airflows: a CFD Study

Jian Hua Zhu, Kian Meng Lim, Bruce R. Gordon, De Yun Wang, Heow Pueh Lee

The effects of anterior ethmoidectomy, alone or combined with antrotomy and uncinectomy, on nasal and sinus airflow patterns were investigated using computational fluid dynamics (CFD) analysis of computed tomography scan-based three-dimensional nasal model reconstructions. The velocity, pressure, and airflow distribution, and airflow pathlines were evaluated. In model I, operated and non-operated airways were compared. In model II, the maxillary sinus was artificially sealed to evaluate the effects of ethmoidectomy alone. For both models, CFD simulations showed that post-op middle meatus airflow patterns were strongly affected, with higher air velocity, lower pressure, and larger-sized vortices, and the overall middle meatus airflow was redistributed laterally into the sinus cavities and away from the septum and superior meatus. Airflow rates at other intranasal sites were unaffected. The increase in post-op maxillary ventilation is larger than those in normal sinuses and sinuses with accessory ostia. Uncinectomy and antrotomy affect only local airflow within the antrum. In conclusion, middle meatus endoscopic sinus surgery (ESS) increases air exchange between sinuses and the nasal airway, increases middle meatus airflow at the expense of superior meatal flow, and produces vortices in the antrum and ethmoid. However, both ethmoidectomy and antrotomy/ uncinectomy affect only local airflow, with negligible influence far from the operation site. These computed changes help us understand where dryness and mucus crusting is likely to occur following middle meatus ESS.

Study of Pre- and Post-Stent Implantation in the Trachea Using Computational Fluid Dynamics

Tzu-Ching Shih, Hung-Da Hsiao, Po-Yuen Chen, Chih-Yen Tu, Tzu-I Tseng, Yung-Jen Ho

Computational fluid dynamics (CFD) allows the visualization and understanding of physics of flow associated with stent implantation. This study uses patient computed tomography (CT) images to investigate the relationship of pressure drop and air flow rate in the tracheal airway. Moreover, the cross-sectional areas of the patient airway were measured and the area stenosis ratios were calculated. The stenosis ratios were 75.64% and 38.08% without and with stent treatment, respectively. Simulation results show that at an air flow rate of 30 L/min, the pressure drops between the inlet and the outlet before and after central airway stent implantation for the inspiratory phase were 77.23 and 7.05 Pa, respectively. The improvement gain (IG) was 9.95. The IG increased with increasing air flow rate. At an air flow rate of 120 L/min, the value of IG was 11.68. A higher IG value indicates lower airway resistance after an airway stent implantation. The CFD numerical results demonstrate the feasibility of computing airway resistance based on CT images. In clinical practice, it is difficult to assess patients with severe airway obstruction using a symptoms score or a pulmonary function test due to their critical condition. The proposed noninvasive approach for determining airway obstruction severity is helpful for patients who are unable to do pulmonary function tests.

Influence of Parameterization on Tracer Kinetic Modeling in DCE-MRI

Roberta Fusco, Mario Sansone, Mario Petrillo, Antonella Petrillo

Tracer kinetic modeling in dynamic contrast-enhanced magnetic resonance imaging (DCE-MRI) is commonly performed using least squares algorithms. The convergence of such algorithms and the repeatability of the estimates are affected by the curvature of the model's expectation surface. An adequate choice of the parameterization can reduce curvature and thus improve parameter estimation. This study analyzes the influence of two parameterizations on the curvature of the Tofts model. The influences of the total acquisition time and the sampling period are evaluated. Analysis results show that using (Ktrans, ve) can significantly reduce the curvature in a large area of the parameter space, suggesting that curvature analysis could guide the choice of the best local parameterization in Gauss-Newton-based algorithms. In addition, increasing the total acquisition time and decreasing the sampling period reduce the curvature. However, only slight improvements are obtained for a total time longer than about 6 min and a sampling period shorter than approximately 10 s. [Coloured figures are available in the on-line version of the manuscript]

Microcirculatory Complexity Responses to the Application of Skin-Surface-Contacting Pressure Stimulation Around Normal Blood Pressure

Hsin Hsiu, Wei-Chen Hsu, Chia-Liang Hsu, Jian-Guo Bau

This study discriminates the microcirculatory responses to the application of pressure stimulation (PS) using approximate entropy (ApEn) analysis to characterize the temporal fluctuations within beat-to-beat laser Doppler signals. Experiments were performed with a control group in which PSs were not applied and with five groups in which PSs of 20, 60, 100, and 160 mmHg were applied, respectively. Each experiment involved making a 20-minute baseline recording and then recording effect data 0-20 minutes (M1) and 50-70 minutes (M2) after stopping skin-surface PS. ApEn and wavelet analyses were performed on the assessed laser Doppler signals. At the pressed site, a significant microcirculatory blood flow (MBF) increase was observed that persisted to M2 only in the 60-mmHg PS group (PS60). The only significant increase in ApEn also occurred in PS60, and the only significant decrease in ApEn occurred in the 100-mmHg PS group. Changes in ApEn can help the identification of the range of PSs that can induce longer-persisting improvements in the MBF. These changes in MBF parameters and ApEn can be attributed to different levels of the pressure-induced vasodilation response. The present findings may aid attempts to improve the local MBF and prevent the occurrence of pressure-associated lesions.

Super Actinic 420 nm Light-emitting Diodes for Estimating Relative Microvascular Hemoglobin Oxygen Saturation

David Townsend, Francesco D'Aiuto, John Deanfield

This paper describes a method for comparing the absorption by hemoglobin of reflected light from a range of high-intensity light-emitting diodes (LEDs) as part of the development of a system to obtain high-contrast video images of microcirculation in vivo coupled with a measurement of the relative hemoglobin oxygen saturation in micro vessels. Light from a range of high-intensity LEDs was used to image oxygenated and deoxygenated hemoglobin in vitro to measure the difference in optical densities. The LED for which the highest difference in optical density was measured was then incorporated in a prototype imaging device with illumination from a super actinic 420-nm LED and filtration of the image at 410 nm and 430 nm. This device produced high contrast-video images of microcirculation at410 nm and 430 nm. The difference in the absorption of light at the two wavelengths allowed the determination of the relative hemoglobin oxygen saturation. The proposed method is shown to be suitable for estimating the relative oxygenated hemoglobin from microvascular images.

Automated Segmentation of Brain Tissue and White Matter in Cryosection Images from Chinese Visible Human Dataset

Min Li, Xiao-Lin Zheng, Hong-Yan Luo, Richard Castillo, Shao-Xiang Zhang, Li-Wen Tan, Edward Castillo, Thomas Guerrero

Cryosection images contain fairly rich and original details of the brain anatomy. Accurate and fast segmentation of cryosection images is of great significance for research of the human brain and development of the Visible Human Project. However, most automated approaches in the literature are designed for magnetic resonance imaging or computed tomography data, and they may not be suitable for cryosection images. Cryosection image segmentation is often realized manually or semi-automatically in practice. The present study proposes an automated algorithm for cryosection image segmentation of brain tissue and white matter and evaluates its accuracy using the Chinese Visible Human (CVH) dataset. This method combines a mathematical morphological approach to delineate brain tissue and k-means clustering to uniquely identify white matter. Firstly, the region of brain tissue is detected coarsely using connected component labeling combined with morphological reconstruction. Then, morphological operations are used for final boundary determination to complete the segmentation of brain tissue. Finally, k-means clustering is employed to extract white matter based on segmented brain tissue. The algorithm was applied to the CVH dataset to automatically extract the entire brain tissue and white matter in the cerebrum, cerebellum, and brain stem. Additionally, the proposed mathematical morphological approach is compared with the region growing method and the threshold morphological method for brain segmentation, and the k-means clustering method is compared with the fuzzy c-means clustering algorithm and the Gaussian mixture model coupled with the expectation-maximization algorithm for white matter extraction. To evaluate performance, a quantitative analysis was conducted using the dice similarity index, false- positive dice, and false-negative dice for comparison with manually obtained segmentation results produced by anatomy experts. Results indicate that the proposed algorithm is capable of accurate segmentation and substantial agreement with the gold standard.

Implementation of Resistance Training Using an Upper-Limb Exoskeleton Rehabilitation Device for Elbow Joint

Zhibin Song, Shuxiang Guo, Muye Pang, Songyuan Zhang, Nan Xiao, Baofeng Gao, Liwei Shi

Most exoskeleton devices for upper-limb rehabilitation are heavy and bulky. The present study develops a light and wearable exoskeleton device for passive and resistance training that can potentially be used in home rehabilitation. A method for implementing resistance rehabilitation based on the proposed upper-limb exoskeleton rehabilitation device is proposed. The method is able to be used commonly in the field of Human-machine force interaction where the machine is of high friction, non-backdrivibility which causes the difficulty to obtain contact force. To verify the efficacy of the method, experiments were conducted under two conditions, namely with passive degrees of freedom unlocked and locked, during elbow flexion and extension. In each case, three levels of resistance were generated and provided to the user. The processed EMG signals can be used to verify that the method is effective in both of cases.

Growth and Differentiation of Osteoblasts Regulated by Low-Intensity Pulsed Ultrasound of Various Exposure Durations

Show-Huie Chen, Chia-Ching Wu, Shyh-Hau Wang, Wen-Tyng Li

Several studies have investigated the effect of low-intensity pulsed ultrasound (LIPUS) on fractured bone and bone cells. In general, positive results were reported, but they may vary depending on the LIPUS operational mode. In the present study, the effect of exposure duration associated with LIPUS insonification on osteoblasts was extensively investigated. In experiments, osteoblasts were insonified with LIPUS of 3, 5, 10, and 20 minutes, respectively. The employed LIPUS used a 1 MHz frequency, a 100 mW/cm2 spatial-average-temporal-average intensity (ISATA), and a 20% duty cycle at a 1 kHz pulse repetition frequency. The effect of LIPUS on osteoblasts was assessed in terms of the growth and differentiation of cells corresponding to cell viability, alkaline phosphatase (ALP) activity, mRNA expression of ALP and osteocalcin (OCN), and Alizarin red-S staining. Results demonstrate that the growth and differentiation of insonified osteoblasts increased with increasing exposure duration for durations of up to 10 minutes. Specifically, with 10 minutes of LIPUS insonification, the proliferation and ALP activity of osteoblasts increased to 1.07- and 1.31-fold than those of the control groups, respectively; OCN mRNA expression and the mineralization of osteoblasts increased respectively to 2.23- and 2.5-fold than those of the control groups. When the exposure duration of LIPUS was further increased to 20 minutes, the growth and differentiation of insonified osteoblasts did not increase. This indicates that the effect of LIPUS insonification on osteoblasts is exposure-duration-dependent. Furthermore, the temperature of the medium corresponding to LIPUS insonfication varied within 0.5 ℃, verifying that the LIPUS insonification provides a non-thermal effect on the regulation of cellular growth and differentiation. Consequently, with appropriate LIPUS exposure duration, the proliferation, differentiation, and mineralization of insonified osteoblasts can be regulated, which could be beneficial for the treatment of bone-related diseases.

2014 Vol. 34, No. 3

Review: Macro-Encapsulation of Islets in Polyvinyl Alcohol Hydrogel

Shoichiro Sumi, Goichi Yanai, Meirigeng Qi, Naoaki Sakata, Zhi Qi, Kaichiang Yang, Yasumasa Shirouzu, Akihiko Hiura, Yuangjun Gu, Kazutomo Inoue

Diabetes mellitus (DM) can be cured by adequate insulin secretion from a relatively small volume of cells. Cell encapsulation enables allo- and even xeno-geneic cell therapy without immunosuppression. Micro-encapsulated islets used in recent clinical trials are not fully retrievable after transplantation. This paper summerizes the development of retrievable and theoretically replaceable macro-encapsulated islets using polyvinyl alcohol (PVA) hydrogel. An aqueous solution of PVA becomes a gel through micro crystallization by freezing and thawing. Utilizing this feature, PVA-macro-encapsulated islets (PVA-MEIs) were developed. Rat islets suspended in Euro-Collins solution containing 3% PVA were encapsulated in a mesh-reinforced PVA hydrogel sheet by freezing and thawing. The feasibility of PVA-MEIs for DM therapy was tested in vitro and in vivo. PVA-MEIs showed glucose-responsive insulin secretion in vitro even after 14-day culture. Rat PVA-MEIs cultured in media containing fresh human plasma showed no morphological changes and maintained insulin content. Intra-peritoneal transplantation of PVA-MEIs containing 750 rat islets ameliorated hyperglycemia in streptozotocin (STZ)-induced diabetic mice to nearly normal levels for up to 30 days with a consistent increase in body weight. Transplantation of PVA-MEIs also prevented metabolic and renal disorders in STZ-induced diabetic mice. PVA-MEIs cryo-preserved for 1, 7, and 30 days showed similar function in vitro and corrected hyperglycemia after intra-peritoneal transplantation in STZ-induced diabetic mice. Intra-peritoneal transplantation of PVA-MEIs containing iso- or allo-geneic islets (approx. 2,000 islets) ameliorated hyperglycemia in STZ-induced diabetic rats in a similar manner for almost half a year although the efficacy gradually decreased with time. Transplantation of PVA-MEIs ameliorated hyperglycemia in diabetic mice and rats without immunosupression. Retrievable and theoretically replaceable PVA-MEIs that can secure cell entrapment can mitigate the potential risks associated with xeno-geneic cells and cells made from undifferentiated cells. Therefore, PVA-MEIs are a promising modality for future DM therapy.

Glycosaminoglycan/Chitosan Hydrogel for Matrix-associated Autologous Chondrocyte Implantation: An In Vitro Study

Fang-Yu Fan, Chien-Chang Chiu, Ching-Li Tseng, Hsuan-Shu Lee, Yung-Ning Pan, Kai-Chiang Yang

Matrix-associated autologous chondrocyte implantation (MACI) is an effective treatment for full-thickness cartilage and osteochondral lesions with encouraging outcomes. However, problems include abnormal growth of chondrocytes during cultivation, cell dedifferentiation, and abnormally regenerated cartilage. A matrix that provides a physicochemical and biological microenvironment for restoring hypertrophic chondrocytes would be beneficial for MACI. Accordingly, this study evaluates the feasibility of using an injectable glycosaminoglycan (GAG)/chitosan hydrogel for MACI. Chitosan gel was prepared and GAGs (hyaluronan and chondroitin-6-sulfate) were added to fabricate a GAG/chitosan matrix. Porcine chondrocytes were isolated from articular cartilage and encapsulated within the GAG/chitosan matrix. Cell viability, material-mediated cytotoxicity, cellular proliferation, collagen production, GAG content, and mRNA gene expression patterns of the chondrocytes were evaluated. The cell viability and material- mediated cytotoxicity assay results show that the GAG/chitosan hydrogel has good biocompatibility. Chondrocytes cultured within the matrix had a slower proliferation but higher GAG production compared to those obtained for a monolayer culture. Real-time polymerase chain reaction results show that the mRNA expression of type II collagen was up-regulated but types I and X collagens were down-regulated. This study demonstrates that incorporating GAGs into a chitosan matrix maintains the normal phenotype of chondrocytes, making the GAG/chitosan matrix a candidate for MACI.

Development of Tracheal Scaffolds Using Hybridization of PLLA Coil Skeleton and Electrospun Structures

Shih-Han Hung, Po-Yueh Chen, Chien-Cheng Tai, Chih-Hung Chou, Wen-Ling Cheng, How Tseng

The larynx and the trachea are critical for respiration, airway protection, and phonation in humans. Ideal methods for the reconstruction of the laryngotracheal structure and restoration of laryngotracheal function once the larynx or/and the trachea has been damaged or removed have not yet been developed. Tracheal tissue engineering has been intensively investigated since the first successful human tracheal transplantation was conducted using decellularized tissue implanted with stem cells in 2008. However, the problem of proximal collapse of the graft has recently emerged and there is thus a need for a structurally strengthened scaffold. In this study, decellularized tissue scaffolds were generated using our previously described detergent-free freeze-dry sonication method. Electrospun mats were designed to form tubes. Direct integration of the decellularized tissue with the electrospun mats was unsuccessful, so a poly-L-lactide (PLLA) coil was designed and successfully combined with the outer electrospun fiber sheath. The results of mechanical tests that involved compressing the tube structure revealed significantly greater mechanical strength for the 3- and 1.5-mm-diameter PLLA coiled tubes compared to that of a native tracheal tube. It is therefore possible to construct a hybrid scaffold consisting of an inner PLLA coil skeleton and an outer sheath of electrospun mats, with the decellularized tissue integrated in between these structures.

Effects of Scaffold-delivered SDF-1 Alpha Protein in Chronic Rat Myocardial Infarction Model

Jiashing Yu, Richard E. Sievers, Randall J. Lee

The delivery of stromal cell-derived factor (SDF)-1 alpha protein via a bioactive scaffold for the repair of chronically damaged myocardium was investigated using in situ tissue engineering. SDF-1 alpha protein, fibrin, or SDF-1 alpha protein in a fibrin matrix were delivered into the myocardium of a rat ischemic cardiomyopathy model five weeks after myocardial infarction (MI). Echocardiography was performed before and five weeks after treatment. The hearts were examined histologically for angiogenesis, infarct size, and stem cell migration. SDF-1 alpha protein alone and fibrin glue both retarded heart function deterioration by recruiting stem cells into the infarcted myocardium and stimulating neovascularization. SDF-1 alpha delivered with fibrin glue recruited the highest quantity of CD34+ in the infarcted area. SDF-1 alpha and fibrin influence the myocardial microenvironment in a chronic MI through the recruitment of stem cells, resulting in arteriogenesis and preservation of left ventricular function. In situ tissue engineering shown to be a viable approach for the treatment of chronic ischemic cardiomyopathy.

Potent Osteogenesis and Chondrogenesis of CD34-Enriched Mouse Adipose-Derived Stem Cells

Yao Xiong, Jing He, Wenjie Zhang, Guangdong Zhou, Yilin Cao, Wei Liu

Adipose-derived stem cells (ASCs) obtained using a widely reported culture method are actually a heterozygous cell population of the adipose stromal vascular fraction (SVF). This heterogeneity may interfere with the multi- differentiation potential of adipose-derived mesenchymal stem cells (ADMSCs). It is therefore necessary to establish an efficient method for isolating ADMSCs that have high multi-differentiation potential. Several studies indicated that mucosialin (CD34) might be one of the specific markers of ADMSCs. In our previous studies, a CD34-enriched cell population sorted from the pooled SVF had stronger differentiation potential than that of unsorted cells in a hair follicle morphogenesis model. However, it remains unclear whether CD34-enriched cells have stronger potential for other lineage differentiation, particularly osteogenesis and chondrogenesis. In this study, CD34+ cells were harvested and sorted from murine adipose-derived cells and their potentials for osteogenesis and chondrogesis were examined using engineered bone and cartilage models. The results show that CD34+ cells exhibited stronger potential for bone formation with stronger van Gieson and collagen I staining than those of CD34— cells and an unsorted SVF when seeded on β-tricalcium phosphate. Furthermore, CD34+ cells also exhibited a much stronger chondrogenic potential than those of CD34— cells and an unsorted SVF, with stronger staining of toluidine blue, Safranin-O, and collagen II in a chondrocyte pellet and engineered cartilage. Most importantly, only CD34+ cells could form a cartilage-like lacunae structure. All these results indicate that CD34 may serve as a specific surface marker for enriching ADMSCs in ASCs.

Synthesis and Properties of Biodegradable Segmented Poly-ε-caprolactone

Ting-Yu Shih, Jean-Dean Yang, Hsi-Wei Jia, Jui-Hsiang Chen

Block copolymers have been used to tune the chemical and physical properties of degradable materials for tissue engineering. In this study, a series of urethane linkages containing segmented poly-ε-caprolactone (sPCL) with various block lengths and weight ratios were synthesized and characterized. The molecular conformations and characteristics of sPCL were investigated using nuclear magnetic resonance, Fourier transform-infrared spectroscopy, and gel permeation chromatography. The effects of the molar ratio and molecular weight of ε-caprolactone precursors on the mechanical properties were studied. The results show that the tensile strength of sPCL, which is tunable, was 35 MPa, much higher than that of a typical PCL sample (16 MPa). In addition, it was found that increasing the number of urethane linkages improves elongation. In vitro studies confirmed that the change of molecular weight of sPCL was significantly accelerated compared to that of homopolymers. These results suggest that sPCL has potential as a tailorable material for implantable devices.

Kinematics of Migration of Individual Fibroblasts in Vitro: Faster in a Group, but More Target-Oriented Alone

Noah Metoki, Roy Asher, Orna Sharabani-Yosef, Amit Gefen

During repair of localized damage in a monolayer of cells, migrating NIH3T3 fibroblasts exhibit certain kinematic traits that are influenced directly by factors in their environment such as temperature, pH, and particularly the numbers and distributions of neighboring cells. The present study measures the velocity and direction of individual fibroblasts cultured in a monolayer during migration into a damaged region. Specifically, a parameter termed “percent ideal walk” was defined for evaluating the efficiency of the migrating cells, which were divided into two distinct groups based on migration behavior, namely those migrating alone or with up to four cells and those migrating in a large group (more than six cells). The results show significantly lower velocities for cells that migrated alone or in a group of up to four cells, compared to the velocity of the cells that migrated in a group of more than seven cells ($p < 0.05$). Interestingly, cells that migrated alone or in small groups showed a trend of more efficient directional migration, which was on the edge of statistical significance ($p = 0.056$). This may be attributed to the abundance of mechanical and chemical stimuli that migrating cells generate and sense in a larger group.

On the Dynamic of UV-Light Initiated Corneal Cross Linking

Jui-Teng Lin, Hsia-Wei Liu, Da-Chuan Cheng

This study models ultraviolet (UV) light photo-initiated cross linking in corneal collagen. Two critical parameters, namely the safety depth (z*) and the cross linking time (T*), are analyzed via both numerical and analytical formulas. z* is shown to be a decreasing function of the molar extinction coefficient and the concentration ( ) of the initiator. A higher light intensity and a smaller initiator concentration require a shorter cross linking time (T*) to achieve a given cross link depth. For = 0.25 and 0.5 mM, the safety depths were z* = 695 μm and 390 μm, respectively. The surface cross linking times for light intensities of 10 and 30 mW were 16 s and to 5.3 s, respectively. However, the volume (z > 0) cross linking time increased with the corneal depth z*. T* (at z = 250 μm) is 2.5 times of the surface value (at z* = 0). Analytical formulas for T* and z* are derived and compared with the numerically fit equation.

Preparation and Characterization of Fe-Au Alloy Nanoparticles for Hyperthermia Application

Ren-Jei Chung, Huey-Yuan Wang, Kou-Ting Wu

Water-dispersible Fe-Au alloy nanoparticles (FA_NPs) for hyperthermia application were synthesized and characterized in this study. From transmission electron microscopy examination, the mean diameter of the FA_NPs was calculated to be 3.9 ± 1.3 nm. The X-ray powder diffraction pattern of prepared FA_NPs shows 2θ peak positions corresponding to pure iron and gold. X-ray fluorescence analysis results show that the FA_NPs were composed of 36.8 wt% iron and 63.2 wt% gold, corresponding to a molecular ratio of iron to gold of 2. Electron spectroscopy for chemical analysis was used to study the binding energies of the atoms. To examine the magnetic properties, superconducting quantum interference device tests were conducted, and field-cooled and zero-field-cooled curves were obtained. The results reveal that the FA_NPs were superparamagnetic at room temperature with a saturation magnetization of 3.5 emu/g. The zeta potential was measured to be -29.8 mV for FA_NPs suspended in deionized water, which indicates good suspension. The in vitro cytotoxicity of the FA_NPs was evaluated using L929 and Hep- G2 cell lines through the WST-8 assay. No significant cytotoxic response was observed for either cell line for concentrations below 10 mg/mL after 24 h of cultivation. Hyperthermia evaluations were carried out with a 1.1-MHz high-frequency induction wave (HFIW) exposure. Each FA_NP was calculated to provide 1.33 × 10-16 J of heat. The viability of the Hep-G2 cell decreased under hyperthermia treatment. The FA_NPs prepared in this study have potential for hyperthermia application.

Bone Regeneration by Lactoferrin in Non-Critical-Sized Rat Calvarial Bone Defects

Tomohiro Yoshimaki, Shuichi Sato, Risa Kigami, Noriko Tsuchiya, Shigeki Oka, Yoshinori Arai, Koichi Ito

Lactoferrin (LF) increases the calcification of the extracellular matrix by osteoblasts, suggesting a potential for LF in bone formation. The present study evaluates the bone regenerative effect of LF in non-critical-sized rat calvarial flat bone defects using in vivo microfocus computed tomography (micro-CT) and tissue sections. Ten 11-week-old male Fischer rats were used. After establishment of general anesthesia, local anesthesia was performed. A horseshoe-shaped skin incision over the head was made, the parietal area was exposed under aseptic conditions, and the periosteum was elevated to expose the bone. Non-critical-sized calvarial bone defects (each 2.7 mm in diameter) were trephined into the dorsal part of the parietal bone on each side of the midsagittal suture. An absorbable collagen sponge permeated with 5.5 mg of LF was placed on the experimental side. A collagen sponge permeated with saline was placed on the control side. Skin closure was accomplished. The day of surgery was designated as day 0. Repeated micro-CT imaging was performed from 1 to 4 weeks after surgery. The defect sites were removed along with surrounding bone and soft tissues, which were stained with hematoxylin and eosin. At 3 and 4 weeks, micro-CT images showed a significant difference in the reossification ratio. Histological analysis revealed more osteoblast-like cells around the bony rim on the LF side than on the control side. LF accelerated bone regeneration in non-critical-sized rat calvarial bone defects, as confirmed by micro-CT and histological analysis.

Efficient Metal Artifact Reduction Method Based on Improved Total Variation Regularization

Zhiwei Tang, Guangshu Hu, Hui Zhang

Metal implants produce strong artifacts in reconstructed computed tomography images and thus severely reduce image quality. This study proposes a method for metal artifact reduction that combines modified compressed sensing reconstruction and the sinogram inpainting method. The procedure starts with total variation reconstruction to obtain an initial image. Then, the image is recovered using improved total-variation-based regularization. This process produces an artifact-free background image. The missing information in the original sinogram is complemented using the forward projection of the background image. Consequently, the transitions between the original sinogram and artificial sinogram are smoothed by re-matching the baseline. The algorithm is validated using simulations and phantom data. Results show that streaks are eliminated and shadows are significantly reduced.

Osteogenesis of Umbilical Mesenchymal Stem Cells in Photo-crosslinked Poly(ethylene glycol)/ε-caprolactone Hydrogels

Shu-Rui Yang, Chan-Kun Chang, Sydney Peng, Chao-Yin Ko, I-Ming Chu

Poly(ethylene glycol) (PEG) was copolymerized with ε-caprolactone and then acrylated to produce photo- crosslinked cell encapsulation hydrogels. The osteogenesis of encapsulated umbilical mesenchymal stem cells (UMSCs) was induced in these hydrogels and PEG hydrogels for comparison. The physical properties of the hydrogel, including the swelling ratio and compressive modulus, were measured. Gel degradation in phosphate buffered saline was also tested. Changes in cell morphology in the hydrogel were examined. Collagen type I gene expression, alkaline phosphatase activity, and calcium deposition were used to evaluate the degree of osteogenesis in the hydrogels. It was found that hydrogels composed of PEG copolymerized with ε-caprolactone are suitable for inducing osteogenesis of UMSCs and thus helpful for bone regeneration.

Effect of Limb Joints and Limb Movement on Intrabody Communications for Body Area Network Applications

MirHojjat Seyedi, Daniel Tze Huei Lai

This study investigates the influence of human body movement on signal attenuation during intrabody communication (IBC) for body area network (BAN) applications. While recent studies have shown channel loss measurements for IBC caused by upper limb mobility, these attenuations have yet to be addressed with respect to both upper and lower body limbs in full-body implementations. In this paper, a number of in vivo experiments are conducted to determine the signal attenuation of the body during IBC. Since limb joints control human mobility, the impacts of the elbow and knee joints within the signal path as well as the effects of joint flexion and extension on signal attenuation are examined. The effects of various natural environments on human body signal transmission are taken into account within a high frequency band (0.3-200 MHz). Results show that the presence of limb joints causes high signal attenuation (up to 8.0 dB). Moreover, the signal attenuation decreases with decreasing joint angle; for example, flexion of the elbow joint resulted in 5.0 dB of signal attenuation at 10 MHz. The results indicate that IBC is most likely to be influenced by movement with frequencies below 50 MHz. Above this, signal attenuation is more influenced by the environment and is less dependent on human body composition, indicating that the signal is less coupled through the body.

Guidance-control-based Exoskeleton Rehabilitation Robot for Upper Limbs: Application to Circle Drawing for Physiotherapy and Training

Wei-Wen Wang, Bing-Chun Tsai, Li-Chun Hsu, Li-Chen Fu, Jin-Shin Lai

Cerebral vascular disease is the leading cause of functional disability among adults. Approximately half of all stroke survivors continue to suffer from severe neurological deficits and hemiparesis in the upper extremities as well as many secondary complications due to immobilization. Robotics can provide highly intensive intervention in stroke rehabilitation as well as an objective means of measuring patient progress. This study designs an upper limb rehabilitation (Rehab) robot with multiple degrees of freedom. This design provides a wider range of motion in 3-dimentional space than that provided by an existing endpoint-fixation system. In addition, unlike cable suspension systems that lack biofeedback, the sensors incorporated into the proposed design can be used to detect the voluntary force produced by the stroke patient. The Rehab robot features an exoskeleton-type design with in-built redundancy, a guidance control system, and force feedback using an electromyographic trigger. Three rehabilitation modes can be selected by physical therapists according to the severity of the patient's upper-limb impairment: passive, active, and guidance. Guidance mode assists patients in motor training, with programs such as drawing circles, which involves complex movements that require coordination between the shoulder and elbow joints. Such skills are ideally suited to relearning functional tasks following a stroke. Physical experiments were conducted in this pilot study to evaluate the performance of the Rehab robot. The results indicate that the robot could be effective. Guidance mode achieves the desired guidance functions, informing the subject of the pose required to complete the task as well as enabling them to reduce unnecessary muscle use.

Effect of Physicochemical Properties of Drugs on Morphology and Release of Microspheres

Zhi-gang Zhang, Ai-ping Sun, Li-xia Long

1,3-bis(-2-chloroethyl)-1-nitrosourea (BCNU)-loaded and paclitaxel-loaded poly(D,L-lactide) (PDLLA) microspheres, respectively, were prepared by the spray-drying method. The influence of the physicochemical properties of the two drugs on the morphology, encapsulation efficiency, and in vitro drug release behavior were studied. The results show that the plasticization of BCNU to PDLLA greatly affects the morphology and release behavior of the microspheres. The microparticles prepared with BCNU had a spherical shape when the initial loading amount was less than 10%. With a further increase in the BCNU loading amount, the microspheres began to aggregate and lost their spherical shape. Compared to paclitaxel-loaded microspheres, BCNU-loaded ones exhibited remarkable burst release behavior due to active macromolecule motion. The cytotoxicity experiments show that the long-term cytotoxicity on tumor cells of BCNU-loaded microspheres was similar to that of paclitaxel-loaded microspheres, and that both the drug loaded in microsphere exhibited a superior inhibition effect on tumor cells to their commercial form.

國內研討會：

- 2014 亞洲生技商機高峰論壇 (2014 BioBusiness Asia Conference)
  會議地點：台北君悅飯店、世貿南港展覽館
  會議時間：2014-07-23~2014-07-24
  網址：http://www.biobusiness-asia.com/2014/

- 2014 生物醫學工程研討會：
  醫學工程專業人員在醫院的定位及工作範疇之探討
  會議地點：台北國壽大樓 B1 國際會議廳
  會議時間：2014-08-15
  網址：http://www.bmes.org.tw/seminar_show.php?id=214

- 第十八屆奈米工程暨微系統技術研討會 NMC 2014
  會議地點：南臺科技大學
  會議時間：2014-08-21~2014-08-22
  網址：http://mech.stust.edu.tw/sysid/mech/nmc2014/Welcome.htm

- 2014 國際奈米科技研討會 (2014 ISNST)
  會議地點：南臺科技大學
  會議時間：2014-10-17~2014-10-18
  網址：http://chem.stust.edu.tw/en/node/2014ISNST

- 2014 科技部工程司醫工學門成果發表會暨生物醫學工程及醫材產業高峰論壇
  會議地點：國立陽明大學
  會議時間：2014-12-13
  網址：暫無

國際研討會：

- The XX Congress of the International Society of Electrophysiology and Kinesiology(ISEK 2014 Biennial Congress)
  Rome, ITALY. July 15-18, 2014.
  http://isekconference2014.com/

- TORONTO'2014: AES-ATEMA 18th International Conference
  Toronto, Canada. August 11-15, 2014.
  http://aestr2014.com/

- The 36th Annual International Conference of the IEEE Engineering in Medicine and Biology Society (EMBC'14)
  Sheraton Hotel & Towers, Chicago, Illinois, USA. August 26-30, 2014.
  http://embc.embs.org/2014/

- 12th International Conference of Numerical Analysis and Applied Mathematics (ICNAAM 2014)
  Rodos Palace Hotel, Rhodes, Greece. September 22-28, 2014.
  http://www.icnaam.org/

- The 1st Global Conference on Biomedical Engineering held with the 9th APCMBE.
  National Cheng Kung University, Tainan, Taiwan. October 9-12, 2014.
  http://conf.ncku.edu.tw/apcmbe9/index.html

- The 16th IEEE International Conference on e-Health Networking, Application & Services (IEEE Healthcom 2014)
  Natal, RN Brazil. October 15-18, 2014.
  http://www.ieee-healthcom.org/index.html

- ISOT 2014 International Symposium on Optomechatronic Technologies
  Seattle, WA USA. November 5-7, 2014.
  https://depts.washington.edu/isot2014/

- MEDICA-World Forum for Medicine - International Trade Fair with Congress
  Dusseldorf, Germany. November 12-15, 2014.
  http://www.medica-tradefair.com/

- International Computer Symposium (ICS 2014)
  Tubghai University, Taichung, Taiwan. December 12-14, 2014.
  http://ics2014.thu.edu.tw/

歡迎會員提供更多研討會相關訊息